In-Building Radio Propagation Characteristics at UHF Frequencies

Seongcheol Kim

School of Electrical Engineering
Seoul National University
Seoul, Korea
e-mail: sckim@maxwell.snu.ac.kr

Abstract

When both the base station and subscriber antennas are located in the cluttered multipath environment inside buildings, fast fading is observed as either antenna is moved over a distance on the order of a wavelength. The fast fading is evident in measurements made on CW signals, on individual arrivals for pulsed excitation, even for pulses as short as 5 ns. The statistical properties of the fading are discussed, along with the usual measures of the pulse response, such as path loss, mean excess delay, rms delay spread and coherence bandwidth.

1. Introduction

Analysis of the radio communication channel characteristics is important for the development of wireless systems such as Personal Communication Systems (PCS), wireless Private Branch Exchanges (wPBX) and wireless Local area Networks (wLAN). Narrow band or CW path loss is a parameter that is used to define the spatial coverage of a base station, while the impulse response parameter such as mean excess delay and rms delay spread are useful in obtaining data rate and the bit error rate. The technical literature has many reports on CW path loss and the impulse response in the 800-900 MHz band and in the 1.3, 1.4 and 1.8 GHz bands [1-13]. Recently we have reported impulse response measurements made in the 2.4 GHz ISM band [20].

It is well known that a portable located in a cluttered environment receives signals arriving from many directions. For CW excitation, the interference between the different arrivals causes the received voltage amplitude to exhibit large spatial variations over distances that are on the order of a half wavelength. If the voltage is sampled at many closely spaced points over a distance of several wavelengths, the sampled values may be treated as a random distribution. When the receiver is obscured from the transmitter, no one signal arrival will be much stronger than many others, and the distribution of voltage amplitudes will approximate a Rayleigh distribution [17] [18]. If a line of sight path exists between transmitter and receiver, the distribution will be Rician [17] [18]. For pulse excitation, some of the individually arriving signals will have relative delay that is less than the pulse width, and can therefore interfere. As a result, the amplitudes of the various pulses can also be expected to exhibit fast fading.

In this paper we examine the fast fading characteristics observed for CW and pulsed signals due to multiple arrivals for propagation inside buildings. When both the transmitter and receiver are located inside a building, the radio link is symmetrical and fast fading is observed when either end of the link is moved. We first show the fast fading phenomena from the measured results and their statistical characteristics. We subsequently consider the fast fading characteristics observed for pulsed signals of 5 ns duration. Even for such short pulses, identifiable pulses in the response are found to exhibit fast fading, indicating the presence of many propagation paths having differences in path length less than 1.5 m.

2. CW Propagation Measurements

The multipath components between transmitter and receiver inside a building are suggested by the ray paths in Figure 1. If the transmitter is held fixed, and the receiver location x_R is varied over a distance on the order of a wavelength, the phases of the arriving rays will also change, resulting in fading of the received signal.

Measurements to confirm the foregoing speculation were made over one floor of a large office building 60.5 m by 44 m using 2.4 GHz CW signals. The large cubicle section in the center of the building is surrounded by rooms of different sizes, some of which are engineering laboratories. The partitions in the cubicle section are 1.57 meters high, while the acoustic drop ceiling was 2.9 meter above the floor. The external walls of this building are made of concrete-blocks and the internal walls of gypsum board on metal studs. The transmitter consists of an RF generator feeding a dipole antenna. The transmitter was located at a cross isle between the cubicles near the center of the main cubicle area at a height of 2.5 meters. The vertically polarized transmitting antenna is usually elevated at the height of 2.75 meter to minimize the obstruction of the Fresnel zone by furniture and other scatterer. The signal

generator transmits a 2.44 GHz continuous sinusoidal wave which corresponds to a wave length of 12.3 centimeter (4.84 inches). The receiver consists of two orthogonally polarized antennas feeding the spectrum analyzer (HP8592A) through an RF switch that can be controlled by a portable computer via its serial port. The receiver is mounted on an industrial cart for easy movement. Two orthogonal polarized receiving antennas were separated 12 inches and placed at a height of 1.27 meters to avoid blockage of the signal path by the industrial cart and the receiver equipment on it.

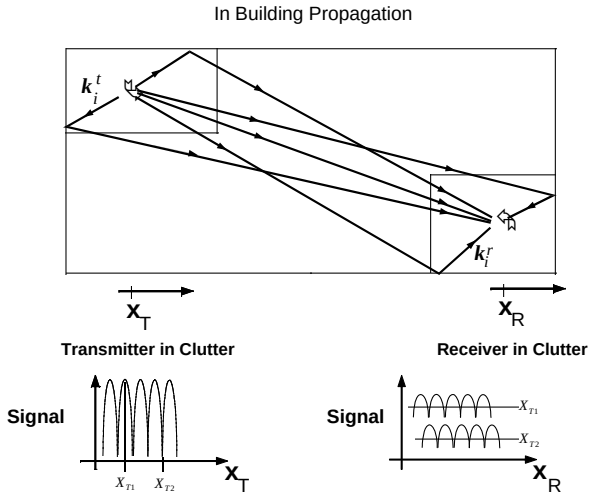

Fig. 1. Cartoon illustrating multipath environments at the transmitter and receiver, both of which are in the clutter.

For the spatial and temporal fading measurements, 300 readings of the received power were collected for each of the two orthogonal polarizations over 110 seconds. The rapid variations of signal level were characterized by the following measurements. At each measurement site, the receiver was located at 24 different positions separated by one quarter wavelength along a straight line. Holding the receiver stationary, 300 data points for both polarizations of the receiving antenna were collected over 110 seconds at each position. Displaying the rapid variation in signal level as a function of time provides the information about temporal fading. Since the receiver was switching between the vertically and horizontally polarized antennas on a very short time scale, it was possible to observe the correlation in the temporal fading between the orthogonal polarizations, which is called an antenna diversity. Averaging the collected data over time at each position and plotting the time average as a function of the receiver position gives the spatial fading characteristics of the signal.

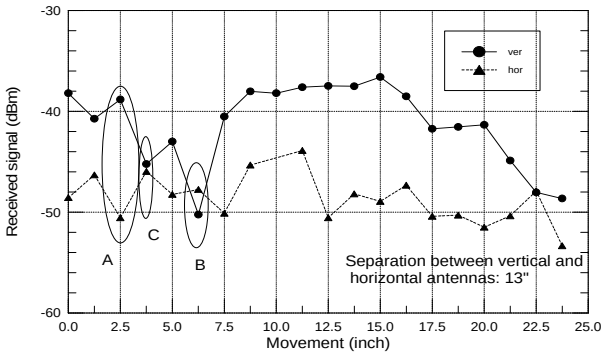

Fig. 2. Spatial fading for a LOS site in the engineering building (24 feet from the transmitter).

Fig. 2 shows the spatial fading of time averaged received signals for both polarizations of the receiving antennas. It is seen that the signals received by two differently polarized antennas generally do not fade at the same position, this allowing for the polarization diversity. The measurements were conducted with the receiver having a line of sight path to the transmitter, so the signal level for the vertical polarization was higher than that for the orthogonal, horizontal polarization, except two positions.

Fig. 3 shows the temporal fading at positions A and B in Fig. 2. It is seen from these curves that the received signal can undergo fades of 10-15 dB over time intervals on the order of a second. In Fig. 3 (a), we find that signal level of the vertically polarized receiver is clearly higher than that of the horizontally polarized receiver. However Fig 3. (b), for which the time averages are nearly the same, show that the polarization corresponding to the higher signal level changes with time. As a result, polarization diversity can be used to remove the fading effect which is due to multipath interference. This observation will be quantified in the following statistical analysis.

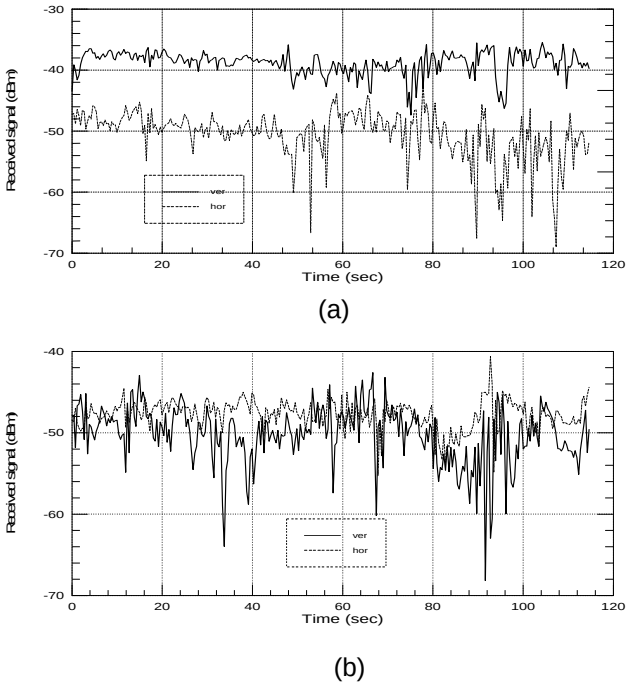

Fig. 3. Temporal fading. (a) and (b) are for positions A and B in Fig. 2, respectively.

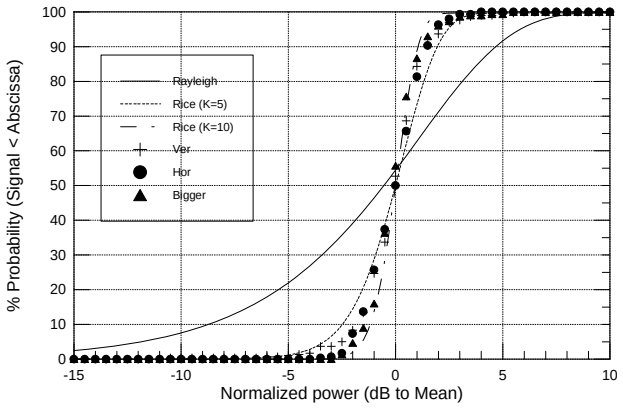

Fig 4. Distribution function of the temporal fading signals with a stationary receiver at the LOS site in the office building

The cumulative distribution function (CDF) of the time varying signal in the engineering building (position C in Fig. 2 (c)) for a line-of-sight path to the transmitter is shown in Fig. 4. The statistical characteristics of multipath fading in this case are similar to the Rician distribution for k value between 5 and 10 for both polarizations, and thus differ significantly from a Rayleigh distribution with the same mean as the measured data. This result suggests that there exists a path that has dominant signal amplitude compared with those of other paths..

3. Impulse Response Measurements

Channel sounding measurements were carried out in two different types of building using 5 ns pulses with a carrier frequency of 2.4 GHz. The first is the same as the CW propagation measurements..

The second building was a large retail store having an open sales floor with storage and facilities rooms at the back of the building. The building is almost square with dimensions 100.5 m by 108.5 m. Both interior and exterior walls are made of concrete blocks except for the 64 m long glass wall at the entrance to the building. The drop ceiling in the sales floor area is made of acoustic tiles and is about 4.27 m above the floor. There is no drop ceiling in the storage room. Two thirds of the sales floor has shelves supported of various heights ranging from 1.82 to 2.3 m, and filled with a variety of metallic and nonmetallic sales items. The other parts of the sales floor have various kinds of metal racks and glass display cases whose heights are from 1 to 1.5 meters. Shelves between 1.82 and 2.44 m high are located in the storage room, and are filled with merchandise up to 3.35 m. The transmitter was placed near the center of the building on the top of a merchandise shelf at a height of 2.95 meters.

A total of 10 receiver sites in the engineering building and 7 sites in the retail store were chosen for measurements. Four sites in the main cubicle area have a Line-of-Sight (LOS) path to the transmitter. For three sites located in the room or the corridor surrounding the main cubicle area, a single wall separated the receiver and transmitter, while at the remaining three sites they were separated by two or more walls. The receiver site located in the engineering laboratory is heavily cluttered by scatterers. In the retail store, four out of five sites on the sales floor had the path to the transmitter obstructed by the merchandise shelves. Two of these sites had light surrounding clutter whose height is comparable to that of the receiving antenna, and another two were heavily cluttered by the merchandise shelves.

At each measurement site, the receiver was located at 16 different positions separated by one quarter wavelength along a straight line. At each position the power delay profile *s(t)* was recorded with the help of a portable computer for subsequent processing. For each type of receiver location (LOS, lightly cluttered, or heavily cluttered), similar results were obtained in both buildings.

4. Overview of Measured Pulse Response

Power delay profiles obtained from measured pulse responses can be separated into three different categories. The first category applies when a LOS path exists between the transmitter and the receiver; the second category consists of lightly obstructed paths; and the third category is for heavily obstructed paths. A series of typical power delay profile *s(t)* for

the 16 receiver locations at a LOS site and at a heavily cluttered site are shown in Figures 5(a), (b).

In Fig. 5(a) it is seen that the power delay profile has a large initial pulse, followed by delayed pulses of small amplitude. Even though LOS conditions exist, the main received pulse is composed of two or more ray arrivals, as evidenced by the spatial fading as the receiver position is moved. Based on the heights of the two antennas and their separation, it appears that the fading is due to interference between the direct and floor reflected rays.

The power delay profiles in Fig. 5(b) for a heavily cluttered site exhibit many individually identifiable peaks whose amplitudes vary rapidly with the location of the receiver.

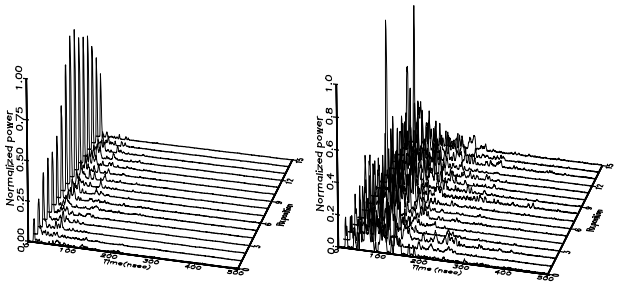

(a) LOS (b) Obstructed

Fig. 5. Individually arriving rays with small relative time delay cause fading of all fingers in the pulse response.

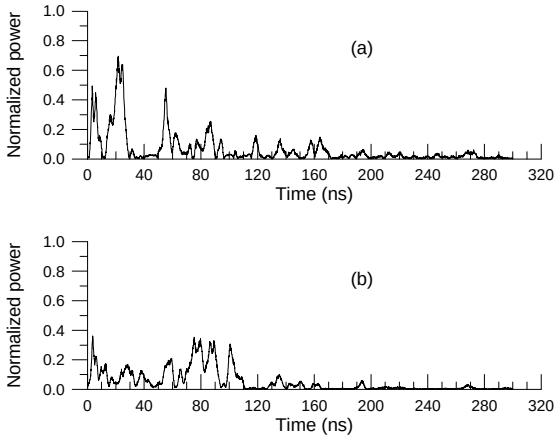

Fig. 6. Power delay profiles for sites with heavily obstructed paths to the transmitter in the engineering building.

This variation is shown more clearly in Fig. 6(a), (b), where we have plotted the power delay profiles obtained at two positions separated by 12.3 cm along the radial direction from the transmitter. In these two figure there exist so many strong pulses that no one pulse dominates the response. The pulse near 20 ns in Fig. 6(a) seems to be the strongest and overlaps with adjacent pulses. The amplitude of this pulse drops so much in Fig. 6(b) that it is believed to be composed of many sub paths. This result can be explained by the postulate that phase differences between these sub paths change with movement of the receiver position, and as a result the amplitude of the superposition of the sub paths also changes. An examination of pulse responses at all of the 16 different receiver positions at this site reveals that none of the pulses have the same amplitude at all receiver positions. In addition to the amplitude variation of the strong pulses, the weak pulses appearing in late time of the response (out to 300 ns) also vary in amplitude as the receiver is moved.

5. Channel Characteristics

Based on the power delay profile it is possible to determine statistical properties of the channel. Several such parameters are obtained below.

5.a. Distribution functions of individual peaks

The measured pulse response contains individual peaks that can be identified throughout the 16 individual receiver positions at each site, but are often jagged. In order to avoid a subjective choice of peak amplitude, and to accommodate all ray arrivals making up a peak we averaged the amplitudes over time bins, whose width is chosen as 6 ns so as to be slightly larger than the 5 ns pulse duration, centered at the delay time T_k In this way, at each receiver position m, we obtain for the time bin centered at T_k an average pulse amplitude $A^2_{k,m}$ [10], [13]. The amplitude $A^2_{k,m}$ is then normalized to the average over the 16 receiver positions.

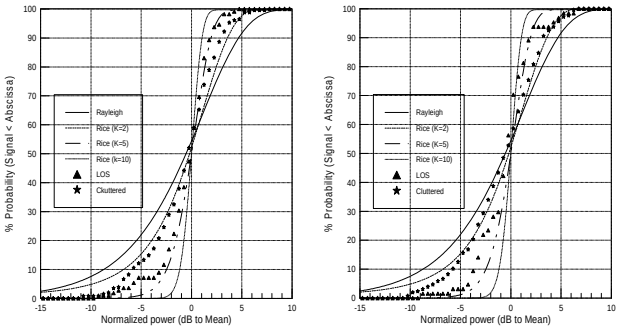

(a) Engineering building (b) Retail store

Fig. 7. Cumulative distributions of peak amplitudes

The normalized amplitudes of individual peaks were aggregated into separate data pools for LOS sites and cluttered sites in the two buildings. Fig. 7 (a) and (b) represents the cumulative distribution functions of the data pools for $A_{k,m}$ corresponding to LOS and cluttered environments in the engineering building and the retail store, respectively. For LOS

paths in both buildings, it is seen from Fig. 7 (a) and (b) that the distribution of peak amplitudes are close to the Rician distribution curve with K = 5, where K is the ratio of the dominant signal to the standard deviation of other weaker and randomly varying signals [20]. At the cluttered sites, the measured distribution seems to follow the Rician curve with $K = 2$, which is very close to the Rayleigh distribution [17], [20]. The differences in the distributions for the LOS and for the cluttered environments is similar to that observed for CW excitation [12].

5.b. Coherence bandwidth

A digital communication system operating in the ISM band can use frequency hopping as a means for mitigating against fast fading. The coherence bandwidth is a measure of the minimum frequency difference such that the signals are not correlated with each other [14], [17]-[19]. If it is assumed that the impulse response represents a complex-valued wide-sense stationary zero mean Gaussian random process, then the frequency coherence of the channel can be found from the auto correlation function. the average power delay profile of the channel for pulse excitation $< s(t) >$. Then the coherence bandwidth can be determined from the measured power delay profiles by taking the Fourier transform

$$R_H(\Delta f) = \int_{-\infty}^{\infty} \langle s(t) \rangle e^{-j2\pi\Delta f\, t}\, dt$$

The coherence bandwidth is then defined as the full width of f at half the maximum of $R_H(f)$.

In Fig. 8 (a) and (b) we have plotted the Fourier transform of the average power delay profile for typical LOS sites and heavily cluttered sites both in the engineering building. The site of the reviver for Fig. 8 (a) has a LOS path to the transmitter and has a power delay profile with only a few additional peaks after the first detectable peak, as in Figure 5 (a). For this case it is seen that the coherence bandwidth is greater than 100 MHz. Fig. 8 (b) is for a heavily cluttered site whose power delay profile contains many late time peaks, as in Fig. 6. The coherence bandwidth at this site is approximately 7 MHz.

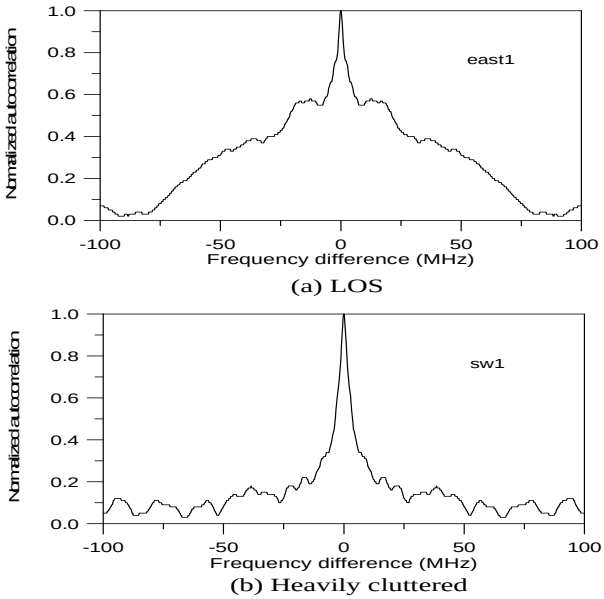

Fig. 8. Fourier transform of the power delay profiles at LOS and heavily cluttered measurement sites

5.c. Mean excess delay and RMS delay spread

In order to calculate the mean excess delay and the rms delay, the noise power was removed from the power delay profile $s(t)$ using the thresholding technique. Table 1 lists the range of values obtained for the mean excess delays and rms delay spread at all sites in the two buildings. For a sites with a LOS path, and even at most sites with lightly obstructed paths to the transmitter, the rms delay is larger than the mean excess delay by about 10 ns. This results from the fact that the power delay profiles in these two environment are dominated by the first few strong pulses in the early time, which heavily influence the mean excess delay, while there are many weak pulses in the late time that influence the rms delay spread. However, at receiver sites having heavily obstructed paths, the rms delay spread and mean excess delay are nearly the same. For this case the power delay profiles are composed of many pulses arriving over about 200 ns, so that pulses arriving long after the early pulses play an important role in determining both quantities [2], [5], [6], [10].

	LOS	Partly Obstructed	Obstructed
Mean Excess Delay	16 - 31 ns	31 - 83 ns	61 - 117 ns
RMS Delay Spread	22 - 43 ns	41 - 74 ns	58 - 90 ns
Coherence BW	36 -100 MHz	6- 30 MHz	5 - 9 MHz

Table 1. Pulse response characteristics

6. Conclusions

The indoor propagation environment generates a rich array of ray paths by connecting the transmitter and receiver. Because of the symmetry of the path when both transmitter and receiver are located in the environmental clutter, multipath interference effects are believed to occur at both ends of the radio link [19]. It is necessary to provide diversity if these effects are to be eliminated. Even for very short pulses, the multipath effect is evident in the various distinguishable pulse arrivals. Our measurements support the widely held belief that the amplitudes of these distinguishable arrivals are Rayleigh distributed for non-LOS links. The measurements of mean excess delay and rms Delay spread at 2.4 GHz are similar to those obtained at lower frequencies.

7. References

[1] D. C. Cox, "Delay doppler characteristics of multipath propagation at 910 MHz in a suburban mobile radio environment," *IEEE Transactions on Antennas and Propagation*, vol. AP-20, No. 5, pp. 625-635, September 1972.

[2] D. M. J. Devasirvatham, "Time delay spread and signal level measurements of 850 MHz radio waves in building environments," *IEEE Transactions on Antennas and Propagations*, vol. AP-34, No. 11, pp. 1300-1305, November 1986.

[3] S. J. Patsiokas, B. K. Johnson, and J. L. Dailing, "Propagation of radio signals inside buildings at 150, 450 and 850 MHz," *Proceedings of the 36th IEEE Vehicular Technology Conference*, Dallas, TX 1986, pp. 66-72.

[4] J. Horikosh, K. Tanaka, and T. Morinaga, "1.2 GHz band wave propagation measurements in concrete building for indoor radio communications," *IEEE Transactions on Vehicular Technology*, vol. VT-35, No. 4, pp. 146-152, November 1986.

[5] A. A. M. Saleh, and R. A. Valenzuela, "A statistical model for indoor multipath propagation," *IEEE Journal on Selected Areas in Communications*, vol. SAC-5, No. 2, pp. 138-146, February 1987

[6] D. M. J. Devasirvatham, "Multipath time delay spread in the digital portable radio environment," *IEEE Communication Magazine*, vol. 25, No. 6, pp. 13-21, June 1987.

[7] Y. Yamaguchi, T. Abe and T. Sekiguchi, "Radio propagation characteristics in underground streets crowded with pedestrians," *IEEE Transactions on Electromagnetic Compatibility*, vol. 30, No. 2, pp. 130-136, May 1988.

[8] H. W. Arnold and R. Murray, D. C. Cox, "815 MHz radio attenuation measured within two commercial buildings," *IEEE Transactions on Antennas and Propagation*, vol. 37, No. 10, pp. 1335-1339, October 1989.

[9] R. Bultitude, S. Mahmoud and W. Sullivan, "A comparison of indoor radio propagation characteristics at 910 MHz and 1.75 GHz, "*IEEE Journal on Selected Areas in Communications*, vol. 7, No. 1, pp. 20-30, January 1989.

[10] T. S. Rappaport, "Characterization of UHF multipath radio channel in factory buildings," *IEEE Transactions on Antennas and Propagation*, vol. 37, No. 8, pp. 1058-1069, August 1989.

[11] T. S. Rappaport, "Indoor radio communications for factories of the future," *IEEE Communication Magazine*, pp. 15-24, May 1989.

[12] J. F. Lafortune, M. Lecours, "Measurement and modeling of propagation losses in a building at 900 MHz," *IEEE Transactions on Vehicular Technology*, vol. 39, No. 2, pp. 101-108, May 1990.

[13] G. L. Turin, F. D. Clapp, T. L. Johnston, S. B. Fine and D. Lavry, "A statistical model of urban multipath propagation," *IEEE Transactions on Vehicular Technology*, vol. VT-21, No. 1, pp. 1-9, February 1972.

[14] A. P. Bello and B. D. Nelin, "The effect of frequency selective fading on the binary error probability of incoherent and differently coherent matched filter receivers," *IEEE Transactions on Communication System*, vol. CS-11, pp. 170-186, June 1963.

[15] Simon Haykin, *Communication Systems*. New York: Wiley, 1983, Chapter 5.

[16] John G. Proakis, *Digital Communications.* New York: McGraw-Hill, 1989, pp. 702-719.

[17] William C. Y. Lee, *Mobile Communications Engineering*. New York: McGraw-Hill, 1982, Chapter 1, 2, 3, and 6.

[18] B. P. Lathi, *Modern Digital and Analog Communication Systems*. Philadelphia: Holt, Rinehart and Winston, 1989, pp. 435-450.

[19] W. Honcharenko, H. L. Bertoni and J. L. Dailing, "Bilateral averaging over receiving and transmitting areas for accurate measurements of sector average signal strength inside buildings," *IEEE Transactions on Antennas and Propagation*, vol. 43, No. 5, pp. 508-512, May 1995.

[20] S. C. Kim, H. L. Bertoni and M. Stern, "Pulse propagation characteristics at 2.4 GHz inside buildings," Accepted for publication in the *IEEE Transactions on Vehicular Technology.*